

Stable UV to IR supercontinuum generation in calcium fluoride with conserved circular polarization states

Philip J. M. Johnson, Valentyn I. Prokhorenko,
and R. J. Dwayne Miller*

*Institute for Optical Sciences and Departments of Chemistry and Physics,
University of Toronto, 80 St. George Street, Toronto, Ontario, M5S 3H6, Canada*
dmiller@lphys.chem.utoronto.ca

Abstract: The supercontinuum generated with a linearly polarized near-IR (775 nm) pump in rotated calcium fluoride is shown to have intrinsic intensity and polarization modulations. To mask the rotation of the crystal plate, we circularly polarize the pump and find greatly improved output parameters for the generated white light: intensity fluctuations of 0.5% limited only by pump laser stability, and a circular polarization state—matching that of the pump—over the entire visible spectrum. This polarization conservation allows the return of the supercontinuum to a linear polarization state or to a pair of linearly polarized beams with correlated intensity fluctuations. We were also able to extend the supercontinuum source deep into the ultraviolet with a frequency doubled (387 nm) pump, to serve as an new source to probe the region where most molecular photochemistry occurs.

© 2009 Optical Society of America

OCIS codes: (320.6629) Supercontinuum generation; (190.7110) Ultrafast nonlinear optics.

References and links

1. R. R. Alfano and S. L. Shapiro, "Emission in the region of 4000 to 7000 Å via four-photon coupling in glass," *Phys. Rev. Lett.* **24**, 584–587 (1970).
2. R. Huber, H. Satzger, W. Zinth, and J. Wachtveitl, "Noncollinear optical parametric amplifiers with output parameters improved by the application of a white light continuum generated in CaF₂," *Opt. Commun.* **194**, 443–448 (2001).
3. P. Tzankov, T. Fiebig, and I. Buchvarov, "Tunable femtosecond pulses in the near-ultraviolet from ultrabroadband parametric amplification," *Appl. Phys. Lett.* **82**, 517–519 (2003).
4. P. F. Tekavec, J. A. Myers, K. L. M. Lewis, and J. P. Ogilvie, "Two-dimensional electronic spectroscopy with a continuum probe," *Opt. Lett.* **34**, 1390–1392 (2009).
5. L. De Boni, C. Toro, and F. E. Hernández, "Pump polarization-state preservation of picosecond generated white-light supercontinuum," *Opt. Express* **16**, 957–964 (2008).
6. H. Hundertmark, S. Rammler, T. Wilken, R. Holzwarth, T. W. Hänsch, and P. St. J. Russell, "Octave-spanning supercontinuum generated in SF₆-glass PCF by a 1060 nm mode-locked fibre laser delivering 20 pJ per pulse," *Opt. Express* **17**, 1919–1924 (2009).
7. C. Nagura, A. Suda, H. Kawano, M. Obara, and K. Midorikawa, "Generation and characterization of ultrafast white-light continuum in condensed media," *Appl. Opt.* **41**, 3735–3742 (2002).
8. M. Ziolk, R. Naskrecki, and J. Karolczak, "Some temporal and spectral properties of femtosecond supercontinuum important in pump-probe spectroscopy," *Opt. Commun.* **241**, 221–229 (2004).
9. K. Midorikawa, H. Kawano, A. Suda, C. Nagura, and M. Obara, "Polarization properties of ultrafast white-light continuum generated in condensed media," *Appl. Phys. Lett.* **80**, 923–925 (2002).
10. A. K. Dharmadhikari, F. A. Rajgara, and D. Mathur, "Systematic study of highly efficient white light generation in transparent materials using intense femtosecond laser pulses," *Appl. Phys. B* **80**, 61–66 (2005).

11. I. Buchvarov, A. Trifonov, and T. Fiebig, "Toward and understanding of white-light generation in cubic media – polarization properties across the entire spectral range," *Opt. Lett.* **32**, 1539–1541 (2007).
12. R. Adair, L. L. Chase, and S. A. Payne, "Nonlinear refractive index of optical crystals," *Phys. Rev. B* **39**, 3337–3350 (1989).
13. V. Kartazaev and R. R. Alfano, "Polarization properties of SC generated in CaF₂," *Opt. Commun.* **281**, 463–468 (2008).
14. A. K. Dharmadhikari, K. Alti, J. A. Dharmadhikari, and D. Mathur, "Control of the onset of filamentation in condensed media," *Phys. Rev. A* **76**, 033811 (2007).
15. D. C. Hutchings, "Nonlinear-optical activity owing to anisotropy of ultrafast nonlinear refraction in cubic materials," *Opt. Lett.* **20**, 1607–1609 (1995).
16. V. I. Prokhorenko, A. M. Nagy, and R. J. Dwayne Miller, "Coherent control of the population transfer in complex solvated molecules at weak excitation. An experimental study," *J. Chem. Phys.* **122**, 184502 (2005).
17. R. S. S. Kumar, K. L. N. Deepak, and D. N. Rao, "Control of the polarization properties of the supercontinuum generation in a noncentrosymmetric crystal," *Opt. Lett.* **33**, 1198–1200 (2008).
18. A. K. Dharmadhikari, F. A. Rajgara, and D. Mathur, "Depolarization of white light generated by ultrashort laser pulses in optical media," *Opt. Lett.* **31**, 2184–2186 (2006).
19. E. C. Carroll, B. J. Pearson, A. C. Florean, P. H. Bucksbaum, and R. J. Sension, "Spectral phase effects on nonlinear resonant photochemistry of 1,3-cyclohexadiene in solution," *J. Chem. Phys.* **124**, 114506 (2006).
20. N. Aközbeke, S. A. Trushin, A. Baltuška, W. Fuß, E. Goulielmakis, K. Kosma, F. Krausz, S. Panja, M. Uiberacker, W. E. Schmid, A. Becker, M. Scalora, and M. Bloemer, "Extending the supercontinuum spectrum down to 200 nm with few-cycle pulses," *New J. Phys.* **8**, 177 (2006).
21. T. Dartigalongue, C. Niezborala and F. Hache, "Subpicosecond UV spectroscopy of carbonmonoxy-myoglobin: absorption and circular dichroism studies," *Phys. Chem. Chem. Phys.* **7**, 1611–1615 (2007).
22. U. Megerle, I. Pugliesi, C. Schrieber, C. F. Sailer, and E. Riedle, "Sub-50 fs broadband absorption spectroscopy with tunable excitation: putting the analysis of ultrafast molecular dynamics on solid ground," *Appl. Phys. B* **96**, 215–231 (2009).
23. W. Liu, S. Petit, A. Becker, N. Aközbeke, C. M. Bowden, S. L. Chin, "Intensity clamping of a femtosecond laser pulse in condensed matter," *Opt. Commun.* **202**, 189–197 (2002).

1. Introduction

Femtosecond supercontinuum light generated in condensed media by intense laser pulses [1] has become an invaluable tool for ultrafast spectroscopy, both as a seed to generate ultrafast broadband laser pulses in optical parametric amplifiers [2, 3] and as a probe source for transient absorption or two-dimensional photon echo spectroscopy [4]. While nearly any dielectric medium—from water [5] to photonic crystal fibres [6]—may be used for white light generation (WLG), crystal plates of sapphire are perhaps the most common source due to sapphire's high thermal conductivity, which negates effects arising from nonlinear absorption. Pumped in the near-IR, supercontinuum generated in a 2 mm thick sapphire plate covers most of the visible spectrum but extends only weakly into the blue (~ 475 nm). To extend deeper into the blue and ultraviolet, crystal plates of the cubic fluoride crystals (e.g. CaF₂ or LiF [7]) must be used for their higher transparency in the UV and small two-photon absorption. The supercontinuum generated in these crystals extends from ~ 350 nm and covers the entire visible range. Unlike sapphire, these crystals must be kept under constant motion to prevent optical damage from the near-IR pump pulses.

Cubic crystals are isotropic in the low fluence regime, and were assumed to generate supercontinuum invariant of crystal orientation. As such, both translation and rotation of the crystal plates have been used to prevent damage during supercontinuum generation [3, 8, 9]. However, recent measurements on crystals undergoing rotation have shown polarization-dependent threshold energies for supercontinuum generation, and depolarization of the supercontinuum due to nonlinear anisotropic birefringence (NAB) induced by intense ultrafast pump pulses [10, 11], as well as intensity modulation in the white light generation as a function of plate orientation [12, 13] or pump polarization orientation [14] due to the $\chi^{(3)}$ properties of cubic media. This can result in an elliptical polarization state for the generated supercontinuum even under linear translation [15].

In this article, we present measurements on femtosecond white light generated in rotated [001]-cut CaF_2 (where the optic axis is collinear with [001] planes) with a linearly polarized pump, documenting modulations in both intensity and polarization state of the generated supercontinuum. We then present a simple and robust method for removing all of the observed instabilities via circularly polarized pumping, and return the generated supercontinuum to a well-defined linear polarization state. Finally, we extend the supercontinuum source deep into the ultraviolet by frequency doubling the pump, while maintaining intensity stability and polarization conservation due to circularly polarized pumping.

2. Instrumentation

The setup for WLG from rotated CaF_2 plates is shown in Fig. 1 below, and is as follows. Linearly polarized ultrafast pulses (150 fs, $\lambda = 775$ nm, 1 kHz repetition rate, see [16] for details) with a beam diameter set to 3 mm by an iris diaphragm pass through a variable OD filter and have the polarization state tuned to circularly polarized by a quarter waveplate (QWP). A 50 mm lens then focuses the pump pulses in a CaF_2 plate (Newlight Photonics Inc., 2 mm thick, [001]-cut, $\lambda/6$ flatness, parallel to within 10 arcseconds) which is kept under constant rotation about the optic axis with a period of four seconds to prevent photodamage, and is very carefully aligned to be normal to the pump. The generated supercontinuum is then collimated by an $f = 20$ mm off-axis parabolic mirror, passes through an achromatic QWP, and is monitored by either a fast photodiode or, for spectral measurements, a commercial grating spectrometer. Threshold energies were determined by detection of light below the pump wavelength (through the use of a cutoff filter) on a photodiode, and pump powers were measured with a semiconductor power meter immediately before the focusing lens. To measure the polarization properties of the supercontinuum, we placed a calcite Glan polarizer in the collimated white light beam.

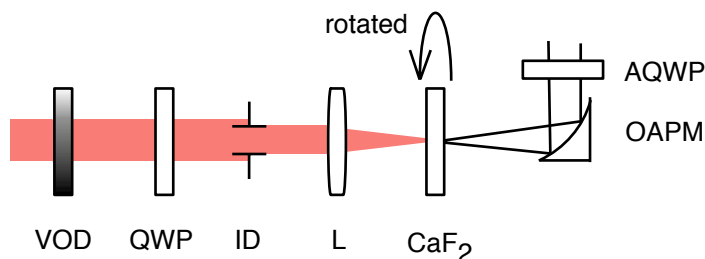


Fig. 1. Schematic of the supercontinuum generation setup. Pump pulses pass through a variable OD filter (VOD), a quarter waveplate (QWP), and an iris diaphragm (ID) before being focussed by a lens L into a calcium fluoride plate. The generated supercontinuum is collected by an off-axis parabolic mirror (OAPM), and sent through an achromatic quarter waveplate (AQWP). For measurements with linearly polarized pump pulses, all QWPs are removed.

3. Modulations and instabilities with a linearly polarized pump

With the optical elements aligned to focus the pump pulse near the far end of the CaF_2 plate (to minimize dispersion) and removal of the QWPs, we observe rotation-dependent supercontinuum generation as in [13]. Above a threshold of $0.96 \mu\text{J}$, the generated white light shows 100% intensity modulations with a period of $\pi/2$ (see Fig. 2a), in agreement with previous observations and attributed to the angular dependence of $\chi^{(3)}$. At orientations where the pump

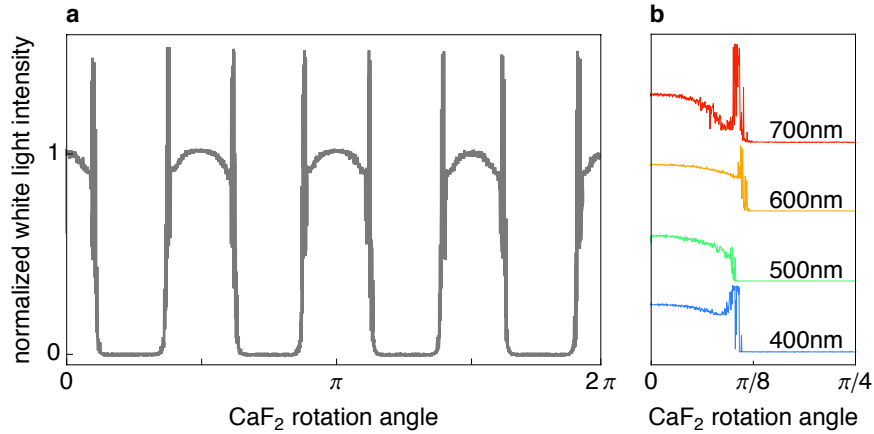


Fig. 2. a) Spectrally integrated intensity of the broadband supercontinuum generated in rotated CaF_2 during one period of rotation (~ 4000 pulses) with a linearly polarized $1.2 \mu\text{J}$ 775 nm pump. Complete modulation in the white light intensity is observed with a periodicity of $\pi/2$, and intense spikes are present at the threshold for white light generation. b) Bandpass filter analysis of the threshold spikes for the $1.2 \mu\text{J}$ pump pulse, each trace normalized to the $\theta = 0$ value. The spectrum is dominated by longer wavelengths, with relatively little contribution in the blue-green.

energy is insufficient to maintain supercontinuum generation, we see intense threshold spikes whose spectral composition is largely red and near-IR (measured with bandpass filters, see Fig. 2b). As the pump pulse energy is increased, we find a disappearance of supercontinuum generation between $1.3 \mu\text{J}$ - $1.6 \mu\text{J}$, and a subsequent return of the white light above $1.6 \mu\text{J}$ with a corresponding increase in the range of orientations under which WLG occurs. At and above this pump power, a red ring surrounding the central white core is prominent (which is apertured out by an iris diaphragm prior to measurement), and the white core itself is free of spatial chirp. For $2.0 \mu\text{J}$ pump pulses we find an ever-present central white spot, and what initially appears to be a more stable ($\sim 20\%$ modulation depth) supercontinuum (see Fig. 3, top panel).

Analysis of the the polarization of the supercontinuum generated by the $2.0 \mu\text{J}$ pump pulse shows the relative stability of the generated supercontinuum is at the cost of a constant polarization state (Fig. 3). Insertion of a Glan polarizer shows supercontinuum with an orientation-dependent polarization state, having both s - and p -polarized components oscillating with a period of $\pi/2$. Following [12], we note $\chi^{(3)}$ for a linearly polarized pump propagating collinear with the $[001]$ planes and polarized at an angle θ with respect to $[100]$ has the form

$$\chi^{(3)}(\theta) = 3\chi_{1122}^{(3)} + (\chi_{1111}^{(3)} - 3\chi_{1122}^{(3)}) \left[\frac{\cos^2(2\theta) + 1}{2} \right]. \quad (1)$$

The nonlinear susceptibility relates to supercontinuum generation through self-focusing [13], a nonlinear optical processes which occurs above a critical incident pump power of

$$P_{cr} = \frac{\lambda^2}{2\pi n_0 n_2}, \quad (2)$$

where n_0 and n_2 are the linear and nonlinear indices of refraction, the latter of which is a function of the nonlinear susceptibility. While the inverse dependence of supercontinuum generation on $\chi^{(3)}$ was only suggestive for measurements where the pump energy oscillated about the

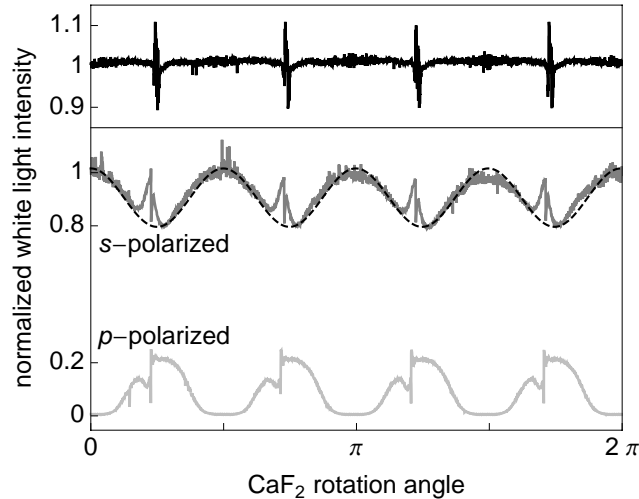


Fig. 3. Polarization analysis of the generated white light for a $2.0\mu\text{J}$ pump pulse (intensity measurement without polarizer shown at top). Both *s*- and *p*-polarized components of the supercontinuum are present and are anti-correlated as a function of rotation. The oscillatory nature of the generated intensity as a function of plate rotation has been attributed to the nonlinear susceptibility, the functional form of which (see Eqs. 1, 2) is shown as an overlay on the *s*-polarized data.

orientation-dependent threshold (as in Fig. 2a for the $1.2\mu\text{J}$ pump), the polarization decomposition of the supercontinuum pumped at $2.0\mu\text{J}$ now shows reasonable agreement with the expected response (see dashed line in Fig. 3).

Given the varying polarization state in the generated supercontinuum, a more careful analysis of the polarization of the supercontinuum is necessary. This is particularly true given that previous measurements of the white light generated in CaF_2 by a linearly polarized pump showed strong depolarization about the pump wavelength, resulting in a spectrally-dependent elliptical polarization of the generated supercontinuum [11]. Measurements on non-cubic materials such as KDP [17] and BK7 [18] show a decoupling of the pump and supercontinuum polarization states, while other less ordered materials (e.g. water [5]), may preserve the polarization state. This can be quantified through the use of the polarization ratio, defined as [11, 17]

$$\rho(\lambda) = I_s(\lambda)/I_p(\lambda), \quad (3)$$

where the intensity is measured for both *s*- and *p*-polarizations by rotation of a Glan polarizer. Shown in Fig. 4, the measured polarization ratio (dark line) and the supercontinuum spectrum (light line) integrated over one complete rotation with a linearly polarized pump shows $\rho \approx 10$ over the entire white light spectrum. The spectrum is slightly narrowed due to the application of a BK7-based cutoff filter to remove spectral components from the near-IR pump, which also decreases the amplitude of spectral components below 380 nm. In addition, we see no strong wavelength-dependent depolarization of the white light, in contrast with [11]. Differences between these two studies, in particular variations in the focusing lens, beam diameter, thickness of the CaF_2 plate, and pump pulse energy required to initiate WLG, preclude any detailed explanation as to why.

Finally, we note that irreversible damage to the CaF_2 plate occurs on a timescale of ~ 1 hour for pump pulse energies $\geq 2.0\mu\text{J}$ having a linear polarization state, despite constant rotation.

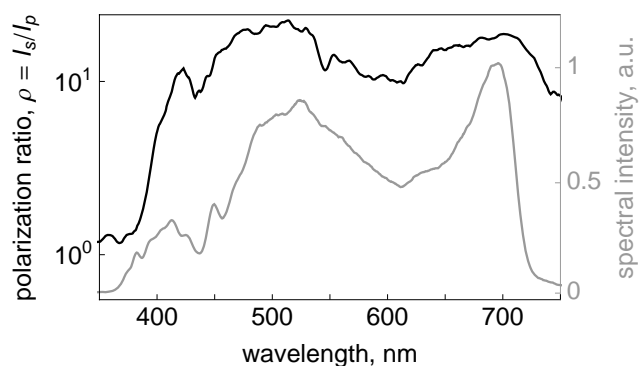


Fig. 4. Measured polarization ratio and white light spectrum integrated over one period of rotation for a linearly polarized $2.0\mu\text{J}$ pump pulse. A ratio of $\rho \approx 10$ is measured, and no strong wavelength-dependent trend in depolarization is observed.

4. Modulation-free supercontinuum generation with a circularly polarized pump

As all of the observed modulations in the supercontinuum generated with a linearly-polarized pump followed from crystal plate rotation, we decided to generate supercontinuum with a circularly polarized pump with the intent of circumventing effects due to rotation. With the addition of a QWP oriented to give circularly polarized pump pulses, we observe a slightly higher threshold for supercontinuum generation of $1.3\mu\text{J}$. At a pulse energy of $1.6\mu\text{J}$, we observe white light without intensity modulations over the entire rotation of the crystal, in stark contrast with the measurements with a linearly polarized pump (detailed in Figs. 2 and 3). As for a linearly polarized pump, we observe a loss of WLG for pump pulses between $1.8\mu\text{J}$ and $2.3\mu\text{J}$, above which the supercontinuum returns, once again with a surrounding red ring. Measurement of the spectrally integrated intensity of white light generated with a circularly polarized $1.6\mu\text{J}$ pump shows (see Fig. 5) a standard deviation from the mean of $\sigma = 0.5\%$ (limited by pump laser stability), and we observe no permanent damage to the crystal plate under these pump

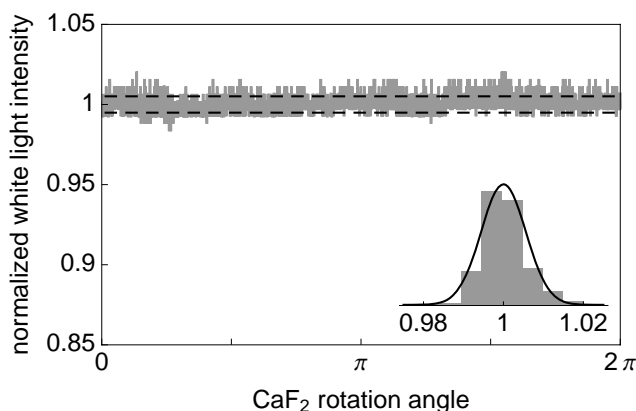


Fig. 5. Spectrally integrated intensity of the broadband supercontinuum generated in rotated CaF_2 during one period of rotation (~ 4000 pulses) with a circularly polarized pump pulse. The standard deviation is 0.5% of the mean, shown as dashed lines. Inset: histogram with Gaussian fit to the distribution.

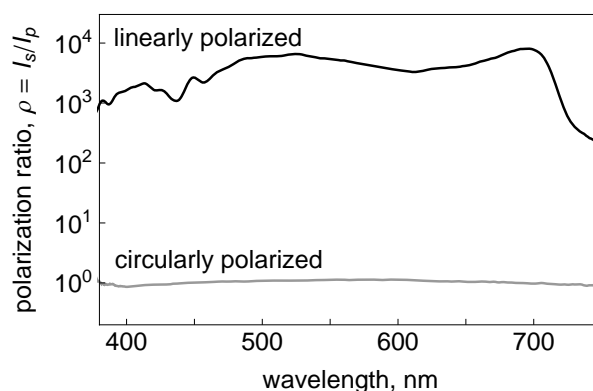


Fig. 6. Polarization ratio for the generated supercontinuum over the entire visible spectrum over one rotation with a circularly polarized pump. A well-defined circular polarization is observed, leading to $\rho = 1$ across the entire spectrum (“circularly polarized” curve). After introducing the AQWP (“linearly polarized” curve), conversion from circular to linear polarization with ratio of $\sim 10^3$ over the entire visible spectrum (380 nm–750 nm) is achieved.

conditions over many hours of continuous use.

While the supercontinuum intensity is stabilized by the circular polarization state of the pump, it was not *a priori* clear that the polarization state for such white light would be well defined, given the results with a linearly polarized pump. However, with the circularly polarized pump, any and all polarization modulations are also observed to disappear. The supercontinuum polarization state now identically mirrors that of the pump, resulting in circularly polarized white light, giving a polarization ratio of $\rho = 1$ over the entire generated spectrum (see Fig. 6, “circularly polarized” curve). Owing to this pump polarization state conservation, the polarization of the supercontinuum can be returned to a linear polarization state with an achromatic quarter waveplate, allowing polarization along any angular orientation of interest. Returning the supercontinuum to an *s*-polarized state, we measure (Fig. 6, “linearly polarized” curve) a polarization ratio of $\sim 10^3$ over the entire visible spectrum, which is consistent with the polarization ratio of a linearly polarized pulse after multipass amplification [18]. The observed decrease in $\rho(\lambda)$ for wavelengths in the near-IR is expected, due to the limited range of the achromatic QWP used (CVI Melles Griot, ACWP-400-700-06-4, 400 nm–700 nm). For applications where the entire generated bandwidth is necessary, it is possible to use calcite or α -BBO Glan-Thompson polarizing beamsplitter cubes to generate a pair of supercontinuum beams at orthogonal polarizations, with the added benefit of having correlated fluctuations between both beams. One obvious application of such pulse pairs is the seeding of a broadband optical parametric amplifier to generate an intense and short broadband pump, while the second of the pulse pairs can be used as a probe line for time-resolved spectroscopy.

5. Interpretation of the stabilizing effect of a circularly polarized pump

We explain these results by interpreting the [001]-cut CaF_2 plate as a kind of polarizer to supercontinuum generation. While linearly polarized pump pulses can generate supercontinuum at lower pulse energies, the intensity modulations having a periodicity of $\pi/2$ matching the cubic crystallinity and nonlinear susceptibility implies the WLG process is less efficient when the pump polarization is not collinear with either the [100] or [010] planes. However, when a circularly polarized pump pulse is incident on the crystal, it has access to the principle crys-

tal axes for all rotation angles, and can thus generate supercontinuum at a constant intensity. Furthermore, while the ratio of threshold energies for linear to circular polarizations was previously noted to be $\sim 2/3$, in only rough agreement with the value for the nonlinear refractive index for CaF_2 responsible for NAB [11], we note that the ratio is simply $1/\sqrt{2}$, the condition necessary for splitting the pump field equally between the two crystal planes, and in excellent agreement with our measured thresholds ($0.96 \mu\text{J}$ and $1.3 \mu\text{J}$ for linear and circularly polarized pumps, respectively). This would also explain the conservation of pump polarization for the generated supercontinuum, where the angular dependence on $\chi^{(3)}$ is now masked by the circularly polarized pump. This unexpected polarization conservation allows the return of the field to a linear polarization state using broadband polarization optics.

6. Deep UV supercontinuum generation with a frequency doubled pump

The increased bandwidth of the supercontinuum generated in CaF_2 by a near-IR pump is a significant gain over sapphire-based sources, but there is still a need for supercontinuum generation deeper in the UV. The vast majority of photochemical processes necessarily occur in the UV, where photon energies can exceed the binding energy of chemical bonds. However, there is currently a dearth of broadband femtosecond UV probe sources (see, e.g. [19]) that do not require few-cycle pump pulses [20]. To extend this source to the deep ultraviolet, the near-IR pump pulses were frequency doubled by a β -BBO crystal cut for second harmonic generation, and a QWP for $\lambda = 387 \text{ nm}$ was employed to again circularly polarize the pump.

We find supercontinuum generation with a circularly polarized 387 nm pump occurs above a threshold value of $1.2 \mu\text{J}$ (slightly below that of the near-IR value), which spans most of the visible range and extends into the deep UV (250 nm - 650 nm), while once again following the pump stability and conserving the circular polarization state. Similar to the near-IR measurements, at higher pump powers a strong blue ring is observed to surround the central blue-white core, while the core itself is free of spatial chirp. As the ultraviolet component of this white light is of interest, a short pass filter (transmitting below $\lambda = 350 \text{ nm}$) is used to isolate the UV supercontinuum from the 387 nm pump, and the measured spectrum is shown in Fig. 7. To return the supercontinuum to a linear polarization, such a wavelength range necessitates α -BBO polarization optics. Alternatively, the circularly polarized supercontinuum in the deep

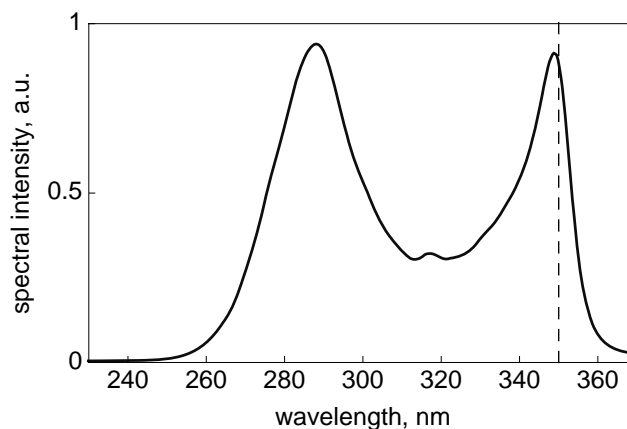


Fig. 7. Measured ultraviolet spectrum of the supercontinuum generated with the second harmonic pump source. A short-pass filter transmitting below $\lambda = 350 \text{ nm}$ (dashed line) is used to remove the pump, and highlight the extension of the white light source into the deep UV.

UV generated with this method may form the basis for ultrafast time-resolved circular dichroism spectroscopy, of particular interest for the studying the rapid dynamics of the secondary structural elements of peptides and proteins [21].

Finally, we note that it should be possible to extend the generated spectrum even further into the deep UV by increasing the thickness of the CaF₂ plates, a trend observed with near-IR pump pulses [22]. With slightly higher pump powers (at the limit for intensity clamping [23]) and thicker CaF₂ crystals, supercontinuum tending into the vacuum UV is likely possible.

7. Conclusion

We have documented supercontinuum generation in calcium fluoride with a linearly polarized pump and fully characterized modulations in intensity and polarization state due to rotation of the crystal plate. The myriad of instabilities observed will preclude the use of such a source for most quantitative spectroscopic applications.

However, as there is a need for increasingly broadband femtosecond supercontinuum sources in the UV, we have introduced a simple method for generating such pulses in rotated calcium fluoride with high stability and a well-defined polarization state through the use of circularly polarized pumping. With a near-IR pump, supercontinuum spanning the entire visible spectrum is generated, ideal for broadband optical parametric amplification in the visible and as a probe for time-resolved spectroscopy. Frequency doubling the pump leads to a supercontinuum source reaching into the deep UV, allowing an increase in the range of molecular systems available for study.

Acknowledgements

Funding for this work was provided by the Natural Sciences and Engineering Research Council (NSERC) of Canada.